From Norbornadiene to Norcamphor and Camphor: Reduced-Cost Semiexperimental Structural Refinement from Limited Isotopologue Data

Lina Uribe,[†,‡] Marco Mendolicchio,[†] Sofia Municio,[¶] Sergio Mato,[¶] Elena R. Alonso,[¶] José L. Alonso,[¶] Iker León,[*,¶] and Vincenzo Barone[*,§]

†*Scuola Normale Superiore di Pisa, Piazza dei Cavalieri 7, 56126 Pisa, Italy*

‡*Scuola Superiore Meridionale, Largo San Marcellino 10, 80138 Napoli, Italy*

¶*Grupo de Espectrocopía Molecular (GEM), Edificio Quifima, Laboratorios de Espectroscopia y Bioespectroscopia, Unidad Asociada CSIC, Parque Científico UVa, Universidad de Valladolid, 47011 Valladolid, Spain*

§*INSTM, via G. Giusti 9, 50121 Firenze, Italy*

E-mail: iker.leon@uva.es; vincebarone52@gmail.com

Abstract

We present an efficient semiexperimental protocol for determining spectroscopically accurate molecular structures from limited isotopologue data, with a focus on medium-sized organic molecules. The availability of all monosubstituted isotopologues of norbornadiene enabled the determination of a complete semiexperimental (r_{eq}^{SE}) equilibrium structure, establishing a reference for validating reduced-dimensionality approaches that avoid deuterium substitution.

The rotational spectrum of norcamphor is reported here for the first time, providing a critical benchmark for assessing the method's accuracy. By combining composite quantum-chemical calculations with a cost-effective vibrational correction scheme, the protocol achieves near-spectroscopic accuracy while substantially reducing computational effort.

This approach enables the structural characterization of large systems where extensive isotopic substitution is impractical, thereby broadening the applicability of semiexperimental methods in modern molecular spectroscopy.

Norcamphor (see Figure 1) is a bicyclic monoterpenoid classified as a bicyclo[2.2.1]heptane according to IUPAC rules.[1] It belongs to the "nor" family—alongside norbornane, norbornene, and norbornadiene (also shown in Figure 1)—which share the same carbon framework as camphor but lack its methyl substituents. While the rotational spectra of norbornane,[2] norbornene,[3] and norbornadiene[4] have long been known, that of norcamphor has remained unexplored until now.

The sizeable dipole moment of norcamphor and the absence of nuclear hyperfine splittings yield a strong and well-resolved rotational spectrum, enabling the detection of ^{13}C and even ^{18}O isotopologues at natural abundance.[5,6] These features have been extensively exploited in the structural characterization of other monoterpenes and monoterpenoids using models such as substitution structures (r_s), ground-state geometries (r_0), and mass-dependent structures (r_m).[4,7–14]

Among the various strategies for gas-phase structure determination, the semiexperimental (SE) approach has emerged as a powerful and more accurate alternative to traditional empirical models.[15–19] By correcting experimental rotational constants with vibrational contributions computed from quantum chemistry, the SE technique yields equilibrium geometries (r_{eq}^{SE}) with spectroscopic accuracy through nonlinear least-squares fitting. However, its application is often hindered by two main limitations: the need for isotopic substitution of all non-equivalent atoms, and the significant computational cost associated with anharmonic vibrational corrections. The first issue can be alleviated by constraining missing parameters to quantum-chemical (QC) values or using mixed regression models.[16,20] To address the second, we have recently introduced a black-box procedure based on energy gradients, which enables the efficient computation of vibrational corrections with minimal loss of accuracy.[21]

In this work, we report the first experimental observation of the rotational spectrum of norcamphor, supported by a computational protocol combining reduced-dimensionality SE refinement with composite quantum-chemical calculations. Our strategy integrates experimental rotational constants from several heavy-atom isotopologues with vibrational cor-

rections computed at modest cost. Due to the lack of observable hydrogen isotopologues at natural abundance, hydrogen coordinates are fixed either from geometries optimized by high-level quantum-chemical methods and/or corrected for the difference between computed and semiexperimental values of norbornadiene. This integrated framework enables accurate structure determination even in the presence of sparse isotopic information and facilitates confident spectral assignments in congested regions.

The family of Pisa Composite Schemes (PCS) has been developed to optimize the accuracy/cost ratio for systems of increasing dimensions. For molecules containing up to around 20 atoms and lacking large static correlation effects, the leading valence contributions to equilibrium geometrical parameters can be estimated accurately by the CCSD(T)-F12b ansatz[22] (CC2) in conjunction with the cc-pVDZ-F12 (2F12) basis set[23–25] and the core-valence (CV) correlation is accounted for by the difference of all-electron (ae) and frozen core (fc) MP2 computations with the cc-pwCVTZ[26] (wC3) basis set:

$$\Delta r^{CV} = r^{(ae-MP2/wC3)} - r^{(fc-MP2/wC3)} \tag{1}$$

Extensive tests of the resulting PCS2 variant[27,28] showed that cheaper approximations can be obtained by considering that the CV contribution is negligible for valence and dihedral angles, while it can be well estimated by a one-parameter function of principal atomic numbers (n_i) for bond lengths.

$$\Delta r_{ij}^{CVB} = -k\sqrt{N_i N_j - 1}\left(r_i^{cov} + r_j^{cov}\right) \tag{2}$$

where $N_i = \min(\mathrm{n_i}, 3)$, r_i^{cov}, r_j^{cov} are covalent radii taken from Ref. 29 and the optimized value of k is 0.0011 for all bonds[30] except CH, where it becomes 0.0021.[28] At the same time, the CC2 valence contribution can be replaced by the significantly cheaper rev-DSD-PBEP86 double hybrid functional[31] in conjunction with a triple-zeta basis set[30] and the D3BJ empirical dispersions[32] (this version is referred to as DPCS3), provided that small

valence corrections (Δr_{ij}^{VB}) are introduced to counterbalance the slight overestimation of delocalization in specific bonds.[33] The resulting variant is denoted BDPCS3, and additional details about Δr_{ij}^{VB} are given in the supplementary information (SI).

Experimental rotational constants, the primary outcomes of rotational spectroscopy, correspond to the vibrational ground state and thus include vibrational averaging. Accordingly, they can be expressed as:

$$B_\tau^0 = B_\tau^{eq} + \Delta B_\tau^{vib} \tag{3}$$

where B_τ^{eq} and ΔB_τ^{vib} denote the equilibrium rotational constant and its vibrational correction along the same principal axis τ. In the framework of second-order vibrational perturbation theory (VPT2) the ΔB_τ^{vib} contributions become explicit functions of quadratic and semi-diagonal cubic force constants,[15,16] which can be effectively computed using the cheap HPCS2 variant (based on the B3LYP functional in conjunction with the 6-31+G* basis set[34] and the D3BJ empirical dispersions[32]) through a low-scaling procedure exploiting analytical gradients.[21,35] Hereafter, rotational constants including vibrational corrections will be denoted by the model used for the computation of equilibrium values followed by //HPCS2.

The characteristics of the different PCS variants are summarized in Table 1.

Table 1: The different PCS variants employed in the present paper. See main text for further details.

Label	**Valence (fc)**	**Δ Core-Valence (ae-fc)**	**Δ Valence (fc)**
PCS2	CCSD(T)-F12b[22]/2F12	MP2/wC3 (see Eq. 1)	none
DPCS3	rev-DSD-PBEP86[31]/3F12$^-$	none	D3BJ[32]
BDPCS3	rev-DSD-PBEP86[31]/3F12$^-$	CVB (see Eq.2)	D3BJ[32] + VB (see Eq. S1)
HPCS2	B3LYP/6-31+G*[34]	none	D3BJ[32]

Vibrationally corrected ground-state constants of different isotopologues yield the so-called semiexperimental (SE) equilibrium rotational constants, which can be used to refine geometrical parameters via least-squares fitting. In the present case, deuterium-substituted isotopologues are not available, preventing direct experimental information on hydrogen po-

sitions. Therefore, C−H bond lengths are estimated independently from quantum chemical computations, possibly corrected by the difference between computed and semiexperimental values for a suitable templating molecule (TM, in the present case norbornadiene). This dual strategy—selective correction of computed bond lengths and template-guided refinement—ensures reliable reconstruction of the hydrogen framework in the absence of isotopic substitution.

In recent works[33] we have compared the equilibrium rotational constants of several molecules including rigid[36] as well as flexible terpenes[37] delivered by different quantum chemical models with their SE counterparts, which have been computed by adding the HPCS2 vibrational corrections to the experimental ground-state rotational constants. The resulting absolute (MAX and MUE) and relative (%MAX and %MUE) maximum and mean unsigned errors revealed that: (*i*) HPCS2 systematically underestimates SE rotational constants by more than 1%, (*ii*) DPCS3 and CC2 achieve average errors around 0.3% and 0.5%, respectively; and (*iii*) PCS2 and BDPCS3 meet the target accuracy of 0.1%. Consequently, PCS2//HPCS2 and BDPCS3//HPCS2 ground state rotational constants are used in this work as accurate reference values for assigning the experimental rotational spectrum of norcamphor.

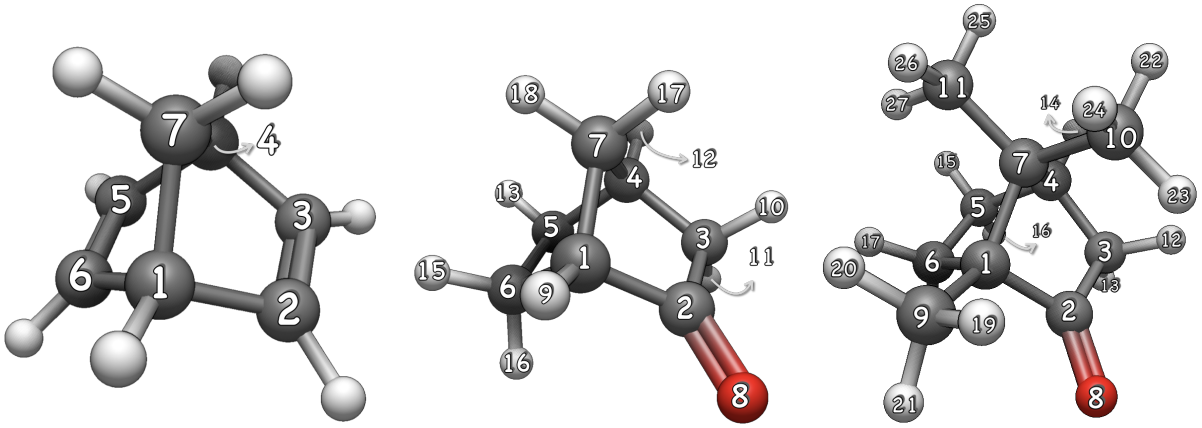

Figure 1: Structure and labelling of norbornadiene, norcamphor, and camphor.

Figure 2 shows the experimental (black lines) and the theoretical spectra of norcamphor

derived from BDPCS3 equilibrium rotational constants, either with (magenta lines) or without (blue lines) HPCS2 vibrational corrections. The agreement between the experimental and the BDPCS3//HPCS2 transitions highlights how this level of accuracy is useful for assigning the experimental spectrum. Therefore, the rotational transitions of norcamphor were identified by starting from the predictions of this model.

The Ray's asymmetry parameter,[38] $\kappa = -0.72$, describes norcamphor as a nearly prolate asymmetric rotor and the QC calculations established that the electric dipole moment has a dominant μ_a component, with considerably smaller μ_b and μ_c components (see Table 2). Consequently, the *a*-type *R*-branch ($\Delta J = +1$), $\Delta K_{-1} = 0$, $\Delta K_1 = +1$, with $K_1 = 0, 1, 2, 3, ..,$ (shortly denoted ${}^aR_{0,1}$) transitions of the parent isotopologue were the first to be observed and assigned by the JB95 software.[39] These transitions are labeled in Figure 2. The regular harmonic pattern can be observed in three groups, each separated by approximately 4000 MHz ($B_0 + C_0$) with each group spanning around 450 MHz ($(B_0 - C_0)(J'' + 1)$, where J'' indicates the lower rotational state[40]). The last group is only partially observed. The *b*- and *c*-type transitions (${}^bR_{\pm1,\pm1}$, ${}^bR_{-1,3}$, ${}^cR_{1,0}$, and ${}^cR_{-1,2}$) were the next to be observed. A total of 30 *R*-branch lines were assigned. As shown in Figure 2, it was also possible to measure *Q*-branch lines ($\Delta J = 0$) of *a*-, *b*-, and *c*-type, specifically were observed ${}^aQ_{0,-1}$, ${}^aQ_{2,-1}$, ${}^bQ_{1,-1}$, ${}^cQ_{1,0}$, and ${}^cQ_{1,-2}$ transitions. A total of 78 lines were assigned and fitted for the parent structure by means of the Pickett's programs (`SPCAT, SPFIT`),[41–44] using the Watson *A* representation and prolate asymmetric rotor.[5,45] The root mean square deviation between measured and fitted positions of those 78 lines was 13 kHz.

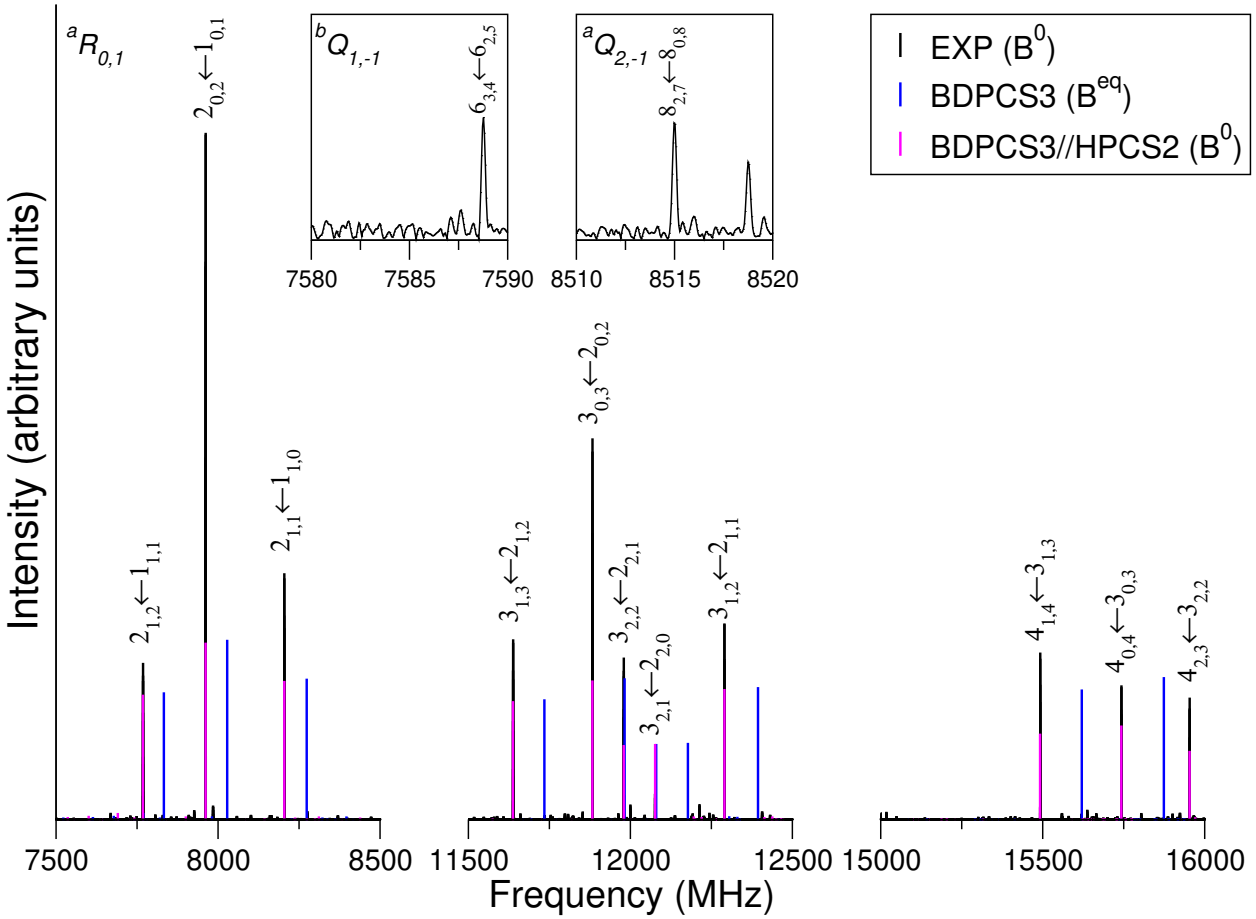

Figure 2: Comparison between the experimental (black lines) and theoretical spectra of norcamphor. The blue lines represent the spectrum derived from BDPCS3 equilibrium rotational constants, while the magenta lines incorporate vibrational corrections at the HPCS2 level. The ${}^{a}R_{0,1}$ progressions are labeled and the ${}^{b}Q_{1,-1}$ and ${}^{a}Q_{2,-1}$ transitions are shown. The full broadband spectrum is shown in Figure S1 of the supplementary information.

Table 2 collects the experimental and computed rotational constants for the parent structure, while Figure 3 shows the experimental (black lines) and the theoretical data derived from equilibrium rotational constants with (magenta lines) or without (blue lines) vibrational corrections.

Table 2: Experimental and computed rotational constants (A_0, B_0, C_0 in MHz), together with HPCS2 vibrational corrections (ΔB_{vib} in MHz), quartic centrifugal distorsion constants in the asymmetrically reduced Hamiltonian (in MHz), and equilibrium electric dipole moment components (μ_{eq}^{τ} in Debye) for norcamphor.

	Parameter	EXP	HPCS2[a] (ΔB_{vib})	MP2[a]	DPCS3[a]	CC2[a]	BDPCS3[a]	PCS2[a]
Parent	A_0	3433.7	3395.7 (31.4)	3406.8	3423.0	3416.6	3436.0	3430.7
	B_0	2105.6	2074.9 (17.8)	2091.0	2097.5	2096.4	2105.7	2104.7
	C_0	1887.6	1860.4 (15.6)	1873.2	1880.4	1878.8	1887.5	1886.4
	MUE[b]		32.0	18.6	8.6	11.7	0.8	1.7
	MAX[b]		38.0	26.8	10.6	17.1	2.3	3.0
	MUE%[b]		1.33	0.75	0.36	0.47	0.03	0.07
	MAX%[b]		1.46	0.78	0.38	0.50	0.07	0.09
	Δ_J	$0.226{\cdot}10^{-3}$	$0.1875{\cdot}10^{-3}$	$0.2098{\cdot}10^{-3}$	$0.2062{\cdot}10^{-3}$	—	—	—
	Δ_K	$0.483{\cdot}10^{-3}$	$0.3925{\cdot}10^{-3}$	$0.6046{\cdot}10^{-3}$	$0.5717{\cdot}10^{-3}$	—	—	—
	Δ_{JK}	$0.1281{\cdot}10^{-3}$	$0.1323{\cdot}10^{-3}$	$0.0070{\cdot}10^{-3}$	$0.0362{\cdot}10^{-3}$	—	—	—
	δ_J	$0.0181{\cdot}10^{-3}$	$0.0155{\cdot}10^{-3}$	$0.0189{\cdot}10^{-3}$	$0.0176{\cdot}10^{-3}$	—	—	—
	δ_K	$0.209{\cdot}10^{-3}$	$0.1338{\cdot}10^{-3}$	$0.1827{\cdot}10^{-3}$	$0.1853{\cdot}10^{-3}$	—	—	—
	$\lvert\mu_{eq}^{a}\rvert$	strong	3.43	3.13	3.21	—	—	—
	$\lvert\mu_{eq}^{b}\rvert$	weak	0.63	0.57	0.70	—	—	—
	$\lvert\mu_{eq}^{c}\rvert$	weak	0.52	0.50	0.52	—	—	—

[a] HPCS2 vibrational corrections to rotational constants, see Eq. 3. [b] Absolute mean and maximum unsigned errors between computed and experimental rotational constants (MUE and MAX in MHz) and the corresponding relative values (MUE% and MAX%).

As previously noted,[46] the HPCS2 equilibrium rotational constants yield results that are closer to the experimental ground-state values than those obtained when vibrational corrections are included (see Table 2 and Figure 3(a)). This behavior arises from a fortuitous error compensation between the neglect of bond lengthening due to vibrational averaging and the systematic overestimation of equilibrium bond lengths at the HPCS2 level. As shown in Figure 3(b), a similar trend is observed for second-order Møller–Plesset perturbation theory (MP2) combined with the 6-311++G** basis set. As a result, these two approaches have become standard practice in spectroscopy, offering a reasonable compromise between accuracy and computational cost. However, this comes at the risk of misleading interpretations of equilibrium geometrical parameters and potential misassignments of experimental data—especially when dealing with closely related structures—as recently illustrated by the case of myrtenol.[36,47,48]

By contrast, the results obtained at the DPCS3 level (see Table 2 and Figure 3(c)) and with CC2 calculations are consistent with those found for other "norcompounds",[36] with

average errors of approximately 0.4 and 0.5%, respectively, when vibrational corrections are included. Finally, both PCS2//HPCS2 and BDPCS3//HPCS2 computations (see Table 2 and Figure 3(d)) achieve the target accuracy of 0.1%.

Norcamphor is a chiral molecule, where all carbon atoms are nonequivalent. Therefore, the signals of the ^{13}C were searched with the help of preliminary BDPCS3//HPCS2 predictions. After observing the ^{13}C isotopologues ($\approx$ 1% abundance), it was clear that signal-to-noise (S/N) ratios of 100:1 could be achieved on the main lines of norcamphor. This suggests that the ^{18}O isotopologue might also be observable, despite its low natural abundance ($\approx$ 0.2%). The transitions $2_{0,2} \leftarrow 1_{0,1}$ for all ^{13}C isotopologues and the transition $2_{1,1} \leftarrow 1_{1,0}$ for ^{18}O are highlighted in Figure 4. The experimental rotational constants for all isotopologues and five quartic centrifugal distortion constants for the parent structure are listed in Table 3 together with the estimated uncertainties. All measured transitions are listed in the Supplementary Information (see Tables S4-S12).

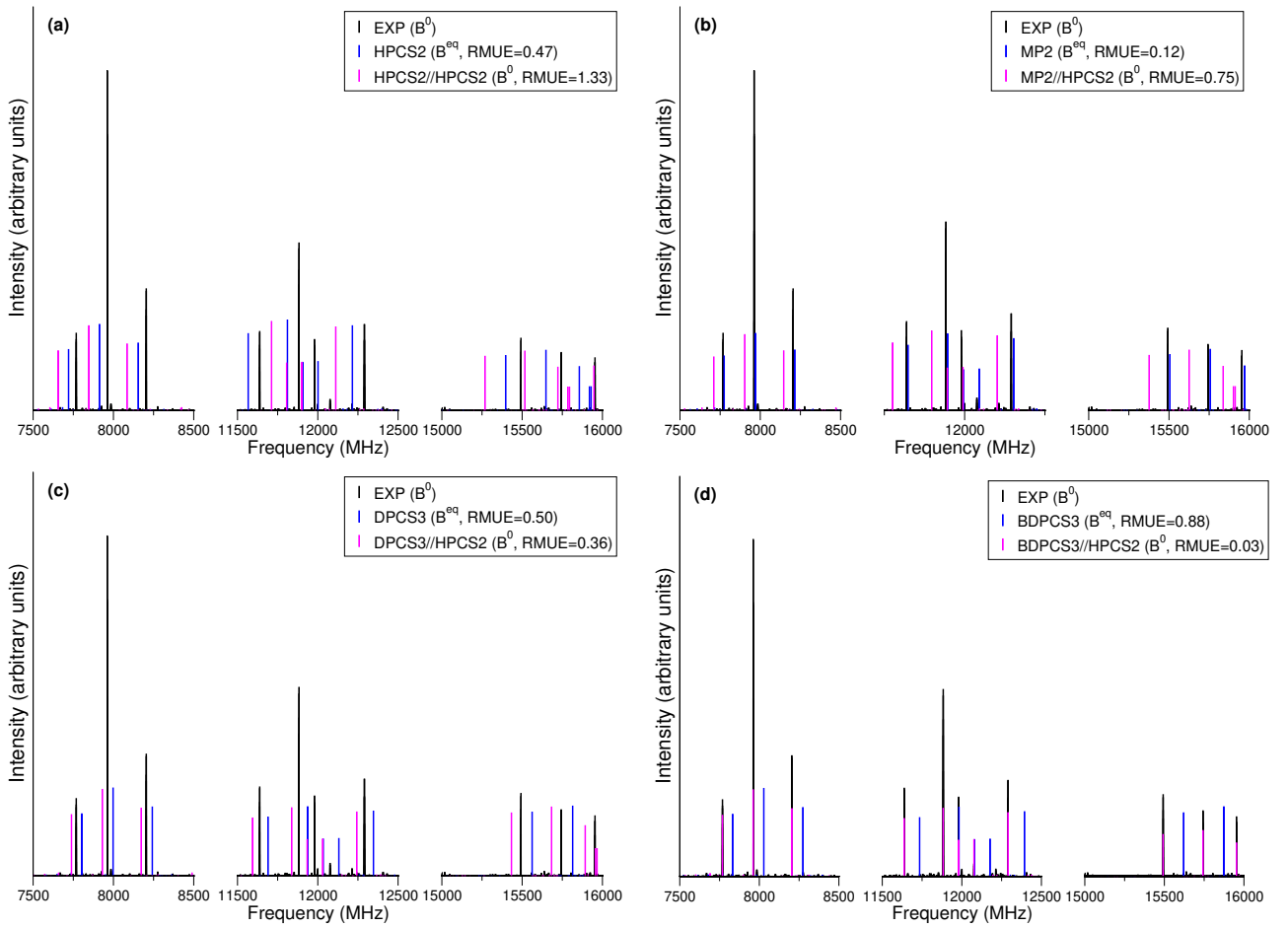

Figure 3: Comparison between the experimental (black lines) and theoretical data of norcamphor. The blue lines represent the spectrum derived from B^{eq}, while the magenta lines incorporate vibrational corrections. Relative maximum unsigned errors between experimental and computed rotational constants (RMUE) are also given. (a) Experimental spectrum vs. HPCS2 and HPCS2//HPCS2 spectra. (b) Experimental spectrum vs. MP2 and MP2//HPCS2 spectra. (c) Experimental spectrum vs. DPCS3 and DPCS3//HPCS2 spectra. (d) Experimental spectrum vs. BDPCS3 and BDPCS3//HPCS2 spectra.

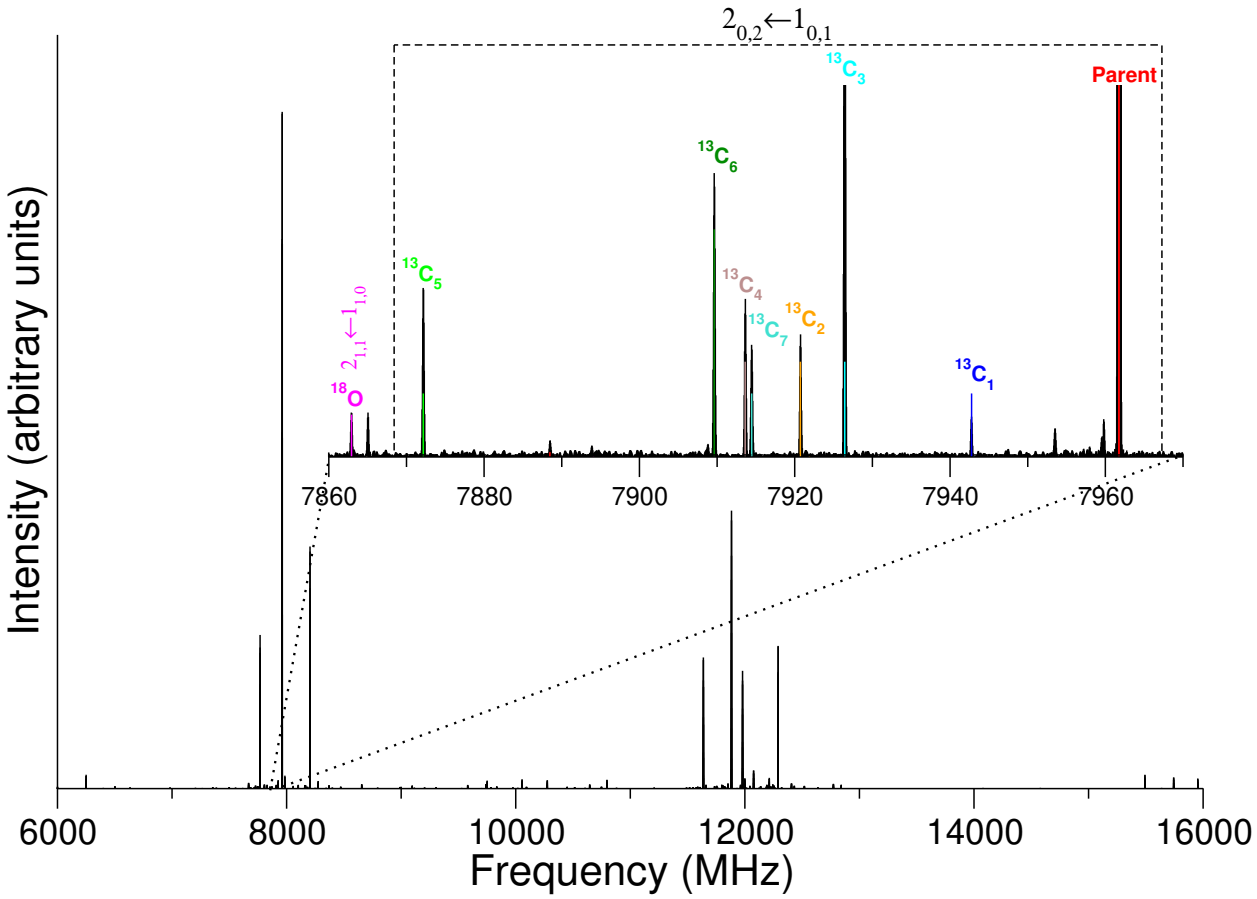

Figure 4: $2_{0,2} \leftarrow 1_{0,1}$ rotational transitions of the ^{13}C isotopologues and $2_{1,1} \leftarrow 1_{1,0}$ transition of ^{18}O isotopologue of norcamphor observed in natural abundance. The labeling follows the atom numbering of Figure 1.

Table 3: Experimental spectroscopic constants (A_0, B_0, C_0, Δ_J, Δ_K, Δ_{JK}, δ_J, and δ_K in MHz) of the parent and singly substituted ^{13}C and ^{18}O isotopologues of norcamphor, in Watson's A-reduced prolate asymmetric rotor Hamiltonian.

	Parent	**^{13}C$_1$**	**^{13}C$_2$**	**^{13}C$_3$**	**^{13}C$_4$**
A_0	3433.68937(123)	3406.4263(51)	3433.3350(48)	3390.779(297)	3410.2746(62)
B_0	2105.60208(110)	2101.6649(40)	2094.0205(34)	2102.8223(76)	2096.4973(48)
C_0	1887.63233(105)	1882.4101(34)	1878.34618(248)	1874.2876(67)	1873.3523(35)
Δ_J	$0.226(37)\cdot10^{-3}$	—	—	—	—
Δ_K	$0.483(54)\cdot10^{-3}$	—	—	—	—
Δ_{JK}	$0.1281(179)\cdot10^{-3}$	—	—	—	—
δ_J	$0.01813(253)\cdot10^{-3}$	—	—	—	—
δ_K	$0.209(40)\cdot10^{-3}$	—	—	—	—
N[a]	78	14	12	12	12
σ[b]	12.96	24.27	20.38	39.66	28.68
	^{13}C$_5$	**^{13}C$_6$**	**^{13}C$_7$**	**^{18}O**	
A_0	3415.808(112)	3386.729(77)	3391.781(308)	3428.1060(56)	
B_0	2077.16668(234)	2098.28492(205)	2084.9016(43)	2015.8886(49)	
C_0	1870.02969(203)	1870.35270(205)	1883.1238(37)	1815.2464(38)	
N[a]	11	11	10	8	
σ[b]	13.01	10.13	23.57	22.96	

[a] Number of measured transitions. [b] RMS deviation of the fit (in kHz).

One major application of high-resolution rotational spectroscopy is the precise determination of molecular geometry. The observed spectra yield the effective rotational constants (A, B, C) for each vibrational state. The structure derived directly from the ground-state constants (A_0, B_0, C_0), measured in this experiment, is referred to as the r_0 structure. As discussed above, much more accurate SE r_{eq} structures can be obtained when there is enough information about the isotopic species. Unfortunately, the rotational constants of norcamphor's parent and its heavy-atom-substituted isotopologues only allow the determination of the r_{eq}^{SE} structure for the heavy-atom backbone. The absence of deuterated species is a common limitation that does not permit determining hydrogen positions.

In order to address this issue, we validated a reduced-dimensionality strategy for norbor-

nadiene, whose ground-state rotational constants have been determined for all monosubstituted isotopologues.[4] These experimental data, combined with computed HPCS2 vibrational corrections, enabled the determination of a complete SE equilibrium geometry. As shown in Table 4, the equilibrium geometries obtained at the BDPCS3 and PCS2 levels already exhibit excellent agreement with their r_{eq}^{SE} counterparts. Further refinement of the heavy-atom positions—while constraining hydrogen bond lengths, valence angles, and dihedral angles to their BDPCS3 or PCS2 values—yielded a reduced-dimensionality SE structure with uncertainty comparable to that of the full-dimensional SE geometry. Moreover, the relative errors in the rotational constants decrease by approximately one order of magnitude when comparing purely theoretical geometries (PCS2 or BDPCS3) with those refined for heavy-atom positions. Although subsequent optimization of hydrogen atom positions leads to a slight improvement in the rotational constants, the gain is marginal and remains within the uncertainty associated with vibrational corrections. This approach thus provides a robust route to derive partial r_{eq}^{SE} equilibrium geometries when only heavy-atom isotopic substitutions are available.

Table 4: Comparison between r_{eq} and r_{eq}^{SE} bond lengths (in Å), valence, and dihedral angles (in degrees) of norbornadiene. The labeling of geometrical parameters follows the atom numbering of Figure 1.

Parameter	r_{eq}					r_{eq}^{SE}[a]				r_{eq}[b]
	HPCS2	**DPCS3**	**CC2**[c]	**BDPCS3**	**PCS2**[d]	**Full(BDPCS3)**	**Full(PCS2)**	**RD(BDCPS3)**[e]	**RD(PCS2)**[f]	**Ref. 4**
$r(C_1-C_2)$	1.5439	1.5362	1.5380	1.5332	1.5348	1.5344(2)	1.53436(6)	1.5338(1)	1.533997(4)	1.5304(31)
$r(C_1-C_7)$	1.5616	1.5529	1.5535	1.5499	1.5502	1.5495(4)	1.5496(1)	1.5504(1)	1.549376(4)	1.5567(28)
$r(C_2-C_3)$	1.3387	1.3369	1.3394	1.3357	1.3365	1.3368(4)	1.3368(1)	1.3364(3)	1.33706(1)	1.3362(30)
$r(C_1-H)$	1.0915	1.0880	1.0871	1.0855	1.0856	1.0844(3)	1.08445(7)	1.0855✓	1.0856✓	1.0903(13)
$r(C_2-H)$	1.0844	1.0811	1.0803	1.0786	1.0790	1.0778(3)	1.07772(6)	1.0786✓	1.0790✓	1.0809(13)
$r(C_7-H)$	1.0948	1.0915	1.0907	1.0890	1.0892	1.0899(3)	1.08865(7)	1.0890✓	1.0892✓	1.0954(12)
$a(C_1-C_2-C_3)$	107.13	107.07	107.06	107.06	107.06	107.06(2)	107.057(4)	107.07(2)	107.0412(4)	107.13(9)
$a(C_1-C_7-C_4)$	92.07	92.25	92.37	92.29	92.37	92.41(3)	92.403(7)	92.33(2)	92.3793(5)	91.90(17)
$a(C_2-C_1-C_6)$	107.40	107.18	107.14	107.18	107.11	107.00(2)	107.036(6)	107.07(2)	107.0575(4)	107.58(25)
$a(C_2-C_1-C_7)$	98.32	98.39	98.38	98.40	98.39	98.42(2)	98.409(4)	98.41(2)	98.4260(5)	98.30(14)
$a(C_1-C_7-H)$	113.24	113.04	112.96	113.03	112.97	112.90(1)	112.956(3)	113.03✓	112.97✓	117.66(26)
$a(C_3-C_2-H)$	128.19	127.94	127.88	127.95	127.88	127.89(3)	127.889(6)	127.95✓	127.88✓	127.84(10)
$a(H-C_7-H)$	110.74	111.25	111.41	111.25	111.38	111.57(4)	111.402(9)	111.25✓	111.38✓	111.99(14)
$d(C_4-C_7-C_1-C_2)$	54.54	54.44	54.42	54.44	54.40	54.35(1)	54.369(3)	54.38(1)	54.3831(3)	—
$d(C_1-C_2-C_3-H)$	176.51	176.40	176.33	176.44	176.31	176.48(4)	176.31(1)	176.44✓	176.31✓	175.94(28)
σ[g]						0.004	0.010	0.001	0.006	
MAX%[h]	1.20	0.30	0.47	0.04	0.07	0.0015	0.0004	0.0068	0.0031	
MAE%[i]	1.41	0.37	0.52	0.11	0.10	0.0006	0.0001	0.0016	0.0011	

[a] The symbol ✓ denotes parameters kept fixed at their guess value. [b] Near equilibrium geometry taken from Ref. 4. [c] CCSD(T)-F12b/cc-pVDZ-F12 structure, the data was taken from Ref. 36. [d] Data taken from the molecular database[49] (https://www.skies-village.it/databases/). [e] Reduced-dimensionality (RD) SE structure obtained starting from the BDPCS3 geometry, with SE rotational constants based on vibrational corrections at the HPCS2 level. [f] Reduced-dimensionality (RD) SE structure obtained starting from the PCS2 geometry, with SE rotational constants based on vibrational corrections at the HPCS2 level. [g] Standard deviation of the fit (in MHz). [h] Maximum absolute percentage error in the rotational constants (for all isotopic species) of the refined structure relative to their experimental counterparts. [i] Mean absolute percentage error in the rotational constants (for all isotopic species) of the refined structure relative to their experimental counterparts.

Table 5 compares the results obtained using different quantum chemical models with those derived either from partial SE optimizations—where CH bond lengths, HCC valence angles, and CCCH dihedral angles were fixed at their BDPCS3 or PCS2 values—or from a modified approach in which the BDPCS3 values for the C_1-C_7, C_1-H_9, C_4-H_{12}, C_7-H_{17}, and C_7-H_{18} bond lengths were corrected by the difference between BDPCS3 and SE values in norbornadiene (the r_{eq}^{TM} structure).

As mentioned above, the remarkable accuracy of the BDPCS3 and PCS2 equilibrium geometries is evidenced by the small deviations between theory and experiment for all available rotational constants, which remain well within the 0.1% target. A reduced-dimensionality SE approach limited to heavy atoms, combined with PCS2 or BDPCS3 hydrogen positions, yields a structure with geometrical parameters falling within fully satisfactory uncertainty ranges. Conversely, the r_{eq}^{TM} structure results in slightly larger deviations relative to the r_{eq}^{SE}

structure, although these remain within spectroscopic accuracy.

For comparison, we also computed the so-called substitution structure (r_s), in which equilibrium atomic positions are estimated from changes in the moments of inertia between isotopologues via the Kraitchman equations, under the assumption that molecular geometry remains unchanged upon isotopic substitution. These calculations were performed using the KRA program, available through the PROSPE database.[44] The resulting structural parameters (see Table 5) are affected by substantial errors, partly due to the large uncertainties associated with very small principal coordinates of certain atoms (see subsection 5.2 in the SI).[7]

Table 5: Comparison between r_{eq}, r_{eq}^{SE}, r_{eq}^{TM}, r_0, and r_s bond lengths (in Å), valence, and dihedral angles (in degrees) of norcamphor. The labeling of geometrical parameters follows the atom numbering of Figure 1.

Parameter	r_{eq}					r_{eq}^{SE}[a]		r_{eq}^{TM}[b]	r_0	r_s
	HPCS2	**DPCS3**	**CC2**[c]	**BDPCS3**	**PCS2**[d]	**RD(BDCPS3)**[e]	**RD(PCS2)**[f]	**BDPCS3**[g]	**BDPCS3**	
$r(C_1-C_2)$	1.5242	1.5189	1.5209	1.5161	1.5176	1.51479(7)	1.51777(9)	1.5161✓	1.51863(9)	1.530 (18)
$r(C_1-C_6)$	1.5591	1.5495	1.5502	1.5465	1.5469	1.54524(7)	1.54707(9)	1.5465✓	1.54908(9)	1.526 (11)
$r(C_1-C_7)$	1.5456	1.5380	1.5392	1.5350	1.5360	1.53375(7)	1.53618(9)	1.5379(5)	1.53759(9)	1.506 (17)
$r(C_2-C_3)$	1.5373	1.5318	1.5340	1.5289	1.5305	1.52764(7)	1.53067(9)	1.5289✓	1.53148(9)	1.597 (18)
$r(C_2-O_8)$	1.2141	1.2084	1.2084	1.2057	1.2064	1.20445(7)	1.20658(9)	1.2057✓	1.20829(9)	1.1873 (41)
$r(C_3-C_4)$	1.5436	1.5355	1.5368	1.5325	1.5336	1.53128(7)	1.53379(9)	1.5325✓	1.53512(9)	1.540 (10)
$r(C_4-C_5)$	1.5474	1.5393	1.5406	1.5363	1.5373	1.53508(7)	1.53749(9)	1.5363✓	1.53892(9)	1.545 (29)
$a(C_1-C_2-C_3)$	105.85	105.84	105.92	105.84	105.91	105.949(5)	105.863(6)	105.84✓	106.146(6)	102.4 (7)
$a(C_1-C_2-O_8)$	127.52	127.54	127.51	127.54	127.50	127.645(5)	127.450(6)	127.54✓	127.841(6)	132.4 (15)
$a(C_2-C_3-C_4)$	102.15	102.10	102.02	102.10	102.03	102.195(5)	101.979(6)	102.10✓	102.392(6)	101.6 (5)
$a(C_2-C_1-C_6)$	105.15	104.89	104.86	104.89	104.85	105.007(5)	104.799(6)	104.89✓	105.204(6)	100.9 (6)
$a(C_2-C_1-C_7)$	101.12	101.17	101.09	101.17	101.10	101.270(5)	101.044(6)	101.17✓	101.467(6)	
$a(C_3-C_4-C_5)$	108.29	108.18	108.11	108.18	108.11	108.307(5)	108.055(6)	108.18✓	108.504(6)	107.0 9)
$d(C_1-C_2-C_3-C_4)$	-3.28	-3.57	-3.55	-3.58	-3.55	-3.621(2)	-3.545(2)	-3.58✓	-3.705(3)	-8.7 (12)
$d(C_3-C_2-C_1-C_6)$	73.20	73.50	73.48	73.51	73.49	73.473(2)	73.497(2)	73.51✓	73.3889(3)	
$d(C_3-C_2-C_1-C_7)$	-31.81	-31.50	-31.51	-31.50	-31.50	-31.535(2)	-31.496(2)	-31.50✓	-31.619(3)	
$d(C_4-C_7-C_1-C_6)$	-53.93	-54.89	-54.87	-54.89	-54.86	-55.20(2)	-54.70(2)	-54.89✓	-55.72(3)	-54.9 (7)
$d(C_7-C_1-C_2-O_8)$	149.21	149.46	149.45	149.41	149.45	149.374(2)	-149.459(2)	149.46✓	149.290(3)	139.6 (17)
σ[h]						0.05	0.05	0.20	0.07	
MAX%[i]	1.33	0.36	0.47	0.03	0.07	0.032	0.031	0.085	0.032	
MAE%[l]	1.46	0.38	0.50	0.07	0.09	0.005	0.006	0.026	0.007	

[a] The C−H, C−C−H, and C−C−C−H parameters are reported in Table S2. [b] Template molecular structure, with norbornadiene as TM. The template bonds are: C_1-C_7, C_1-H_9, C_4-H_{12}, C_7-H_{17}, and C_7-H_{18}, which correspond to the bridge atoms. [c] CCSD(T)-F12b/cc-pVDZ-F12 structure, the data was taken from Ref. 36. [d] Data taken from the molecular database[49] (https://www.skies-village.it/databases/). [e] Reduced-dimensionality (RD) SE structure obtained starting from the BDPCS3 geometry, with SE rotational constants based on vibrational corrections at the HPCS2 level.[f] Reduced-dimensionality (RD) SE structure obtained starting from the PCS2 geometry, with SE rotational constants based on vibrational corrections at the HPCS2 level. [g] $r_{eq}^{TM} = r(\mathrm{BDPCS3}) + \Delta TM$; $\Delta\mathrm{TM} = r_{eq}^{\mathrm{SE}}(\text{full BDPCS3}) - r_{eq}(\mathrm{BDPCS3})$. [g] Standard deviation of the fit (in MHz). [i] Maximum absolute percentage error in the rotational constants (for all isotopic species) of the refined structure relative to their experimental counterparts. [l] Mean absolute percentage error in the rotational constants (for all isotopic species) of the refined structure relative to their experimental counterparts.

The accuracy of the reduced-dimensionality SE approach based on BDPCS3 values, to-

gether with the development of cost-effective procedures for evaluating vibrational corrections, prompted us to revisit the case of camphor. The size of this molecule, combined with the lack of deuterium substitutions, had previously hindered the application of SE techniques using conventional strategies. As shown in Table 6, the least-squares refinement yields stable and accurate geometrical parameters for all non-hydrogen atoms.

The agreement with the $r_m^{(1)}$ structure reported by Kisiel and co-workers[7] is generally satisfactory, with the notable exception of the C1–C7 bond length. The SE equilibrium value for this parameter is close to the BDPCS3 prediction, and significantly longer than both the r_s and $r_m^{(1)}$ values, which are among the least precisely determined experimental parameters.

Table 6: Comparison between r_{eq}, r_{eq}^{SE}, r_0, and r_s bond lengths (in Å), valence, and dihedral angles (in degrees) of camphor. The labeling of geometrical parameters follows the atom numbering of Figure 1.

Parameter	$\boldsymbol{r_{eq}}$[a]			$\boldsymbol{r_{eq}^{SE}}$[a]	$\boldsymbol{r_0}$	$\boldsymbol{r_s}$
	HPCS2	**DPCS3**	**BDPCS3**	**RD(BDCPS3)**[b]	**Ref. 7**	**Ref. 7**
$r(C_1-C_2)$	1.5317	1.5254	1.5224	1.52219(4)	1.537(10)	1.536(9)
$r(C_1-C_6)$	1.5645	1.5543	1.5512	1.55096(4)	1.557(6)	1.543(7)
$r(C_1-C_7)$	1.5685	1.5571	1.5540	1.5538(4)	1.543(8)	1.518(6)
$r(C_1-C_9)$	1.5149	1.5097	1.5068	1.50657(4)	1.522(4)	1.528(4)
$r(C_2-C_3)$	1.5352	1.5306	1.5276	1.52738(4)	1.530(3)	1.547(11)
$r(C_2-O_8)$	1.2144	1.2090	1.2063	1.20601(4)	1.212(2)	1.207(4)
$r(C_3-C_4)$	1.5422	1.5354	1.5325	1.53222(4)	1.545(5)	1.535(3)
$r(C_4-C_5)$	1.5465	1.5393	1.5363	1.53610(4)	1.547(4)	1.540(3)
$r(C_7-C_{10})$	1.5377	1.5304	1.5275	1.52723(4)	1.542(6)	1.549(4)
$r(C_7-C_{11})$	1.5344	1.5271	1.5242	1.52391(4)	1.534(5)	1.533(5)
$a(C_1-C_2-C_3)$	106.61	106.56	106.56	106.542(2)	105.8(2)	105.4(7)
$a(C_1-C_2-O_8)$	126.91	126.91	126.91	126.888(2)	126.8(1)	129.0(11)
$a(C_1-C_7-C_{10})$	113.20	113.00	113.00	113.000(2)	113.2(4)	113.2(5)
$a(C_1-C_7-C_{11})$	114.15	114.03	114.03	114.025(2)	114.1(6)	114.0(7)
$a(C_2-C_3-C_4)$	101.82	101.73	101.73	101.71(2)	101.6(1)	101.3(6)
$a(C_2-C_1-C_6)$	103.01	103.11	103.11	103.0912(2)	102.6(6)	102.2(14)
$a(C_2-C_1-C_7)$	100.48	100.38	100.38	100.362(2)	100.6(3)	101.1(5)
$a(C_2-C_1-C_9)$	114.69	114.46	114.46	114.439(2)	113.6(6)	112.0(9)
$a(C_3-C_4-C_5)$	106.53	106.49	106.49	106.47(2)	106.5(3)	106.7(3)
$d(C_1-C_2-C_3-C_4)$	0.63	0.39	0.39	0.458(4)	—	—
$d(C_2-C_3-C_4-C_5)$	72.07	72.21	72.21	72.300(4)	—	—
$d(C_2-C_1-C_7-C_{10})$	65.10	64.87	64.87	64.871(4)	—	—
$d(C_2-C_1-C_7-C_{11})$	-171.39	-171.45	-171.45	171.4520(4)	—	—
$d(C_3-C_2-C_1-C_6)$	-70.99	-70.91	-70.91	70.825(4)	—	—
$d(C_3-C_2-C_1-C_7)$	34.02	34.20	34.20	34.284(4)	—	—
$d(C_3-C_2-C_1-C_9)$	163.14	163.19	163.19	163.288(4)	—	—
$d(C_7-C_1-C_2-O_8)$	-146.75	-146.26	-146.26	-146.212(4)	—	—
σ[c]				0.09		
MAX%[d]	1.46	0.41	0.04	0.019		
MAE%[e]	1.58	0.46	0.09	0.005		

[a] The C–H, C–C–H, and C–C–C–H parameters are reported in Table S3. [b] Reduced-dimensionality (RD) SE structure obtained starting from the BDPCS3 geometry, with SE rotational constants based on vibrational corrections at the HPCS2 level. [c] Standard deviation of the fit (in MHz). [d] Maximum absolute percentage error in the rotational constants (for all isotopic species) of the refined structure relative to their experimental counterparts. [e] Mean absolute percentage error in the rotational constants (for all isotopic species) of the refined structure relative to their experimental counterparts.

The discrepancy for the C1–C7 bond is likely attributable to limitations in the experimental determination of this parameter, as previously noted by Kisiel and co-workers,[7] rather

than a failure of the SE approach. On the contrary, the close match with the BDPCS3 prediction suggests that the SE method provides a more realistic equilibrium geometry for this structurally constrained bond. Therefore, in our opinion, the newly obtained SE structure not only confirms the quantum-chemical predictions but also represents a significant improvement over all previous estimates.

This work provides the complete semiexperimental (r_{eq}^{SE}) equilibrium structure of norbornadiene and reports the first high-resolution rotational spectrum of norcamphor, enabling accurate determination of its equilibrium gas-phase geometry. Building on these results, we validated a reduced-dimensionality semiexperimental approach that achieves spectroscopic accuracy without requiring full isotopic substitution.

In particular, hydrogen coordinates—unresolvable at natural abundance—are constrained using either high-level quantum-chemical predictions or transferred from a closely related reference molecule. This template-assisted refinement, combined with a computationally efficient black-box treatment of vibrational effects, enables reliable reconstruction of the full molecular geometry, including all heavy-atom positions.

The methodology presented here offers a transferable and cost-effective framework for accurate structural determination of medium-sized molecules via rotational spectroscopy. Its successful application to both norcamphor and camphor demonstrates its robustness and versatility, paving the way for future extensions to systems with greater functional complexity, stereochemical diversity, or limited experimental data.

Acknowledgement

Funding from Gaussian Inc. is gratefully acknowledged by the Italian authors. The financial funding from Fundacion Universidad Valladolid (PIP 063/227161) is acknowledged. S. Mato has been funded by the call for UVa 2023 predoctoral contracts, co-funded by Banco Santander and by the predoctoral contract of Junta de Castilla y León 2023, co-funded by

the European Social Fund (FSE+).

Supporting Information Available

Additional computational and experimental details. Vibrational corrections at the HPCS2 level for the parent structure and all isotopologues of norbornadiene, norcamphor, and camphor. Z-matrices employed in the SE fitting of norbornadiene, norcamphor, and camphor. DPCS3 equilibrium geometry and r_s structure (Cartesian coordinates). Broadband experimental spectrum. Measured transitions for the parent structure and all the detected isotopologues.

References

(1) Favre, H. A.; Powell, W. H. *Nomenclature of Organic Chemistry*; The Royal Society of Chemistry, 2013; p 163.

(2) Choplin, A. Microwave Spectrum and Dipole Moment of Norbornane. *Chem. Phys. Lett.* **1980**, *71*, 503–506.

(3) Chiang, J. F.; Chiang, R.; Lu, K.; Sung, E.-M.; Harmony, M. D. The Molecular Structure of Norbornene as Determined by Electron Diffraction and Microwave Spectroscopy. *J. Mol. Struct.* **1977**, *41*, 67–77.

(4) Knuchel, G.; Grassi, G.; Vogelsanger, B.; Bauder, A. Molecular Structure of Norbornadiene as Determined by Microwave Fourier Transform Spectroscopy. *J. Am. Chem. Soc.* **1993**, *115*, 10845–10848.

(5) Gordy, W.; Cook, R. L. *Microwave Molecular Spectra*; Interscience Pub., 1984.

(6) Kroto, H. W. *Molecular Rotation Spectra*; Wiley-Interscience Publication, 1975.

(7) Kisiel, Z.; Desyatnyk, O.; Białkowska-Jaworska, E.; Pszczółkowski, L. The Structure and Electric Dipole Moment of Camphor Determined by Rotational Spectroscopy. *Phys. Chem. Chem. Phys.* **2003**, *5*, 820–826.

(8) Neeman, E. M.; Dréan, P.; Huet, T. R. The Structure and Molecular Parameters of Camphene Determined by Fourier Transform Microwave Spectroscopy and Quantum Chemical Calculations. *J. Mol. Spectrosc.* **2016**, *322*, 50–54.

(9) Loru, D.; Bermúdez, M. A.; Sanz, M. E. Structure of Fenchone by Broadband Rotational Spectroscopy. *J. Chem. Phys.* **2016**, *145*, 074311.

(10) Chrayteh, M.; Huet, T. R.; Dréan, P. The Gas-Phase Microwave Spectrum of Sabinene Revisited Reveals New Structural Parameters. *J. Mol. Struct.* **2021**, *1240*, 130515.

(11) Neeman, E. M.; Avilés Moreno, J. R.; Huet, T. R. The Gas Phase Structure of α-Pinene, a Main Biogenic Volatile Organic Compound. *J. Chem. Phys.* **2017**, *147*, 214305.

(12) Neeman, E.; Avilés-Moreno, J.-R.; Huet, T. The Quasi-Unchanged Gas-Phase Molecular Structures of the Atmospheric Aerosol Precursor β-Pinene and Its Oxidation Product Nopinone. *Phys. Chem. Chem. Phys.* **2017**, *19*, 13819–13827.

(13) Marshall, F. E.; Sedo, G.; West, C.; Pate, B. H.; Allpress, S. M.; Evans, C. J.; Godfrey, P. D.; McNaughton, D.; Grubbs II, G. The Rotational Spectrum and Complete Heavy Atom Structure of the Chiral Molecule Verbenone. *J. Mol. Spectrosc.* **2017**, *342*, 109–115.

(14) Chrayteh, M.; Dréan, P.; Huet, T. R. Structure Determination of Myrtenal by Microwave Spectroscopy and Quantum Chemical Calculations. *J. Mol. Spectrosc.* **2017**, *336*, 22–28.

(15) Pulay, P.; Meyer, W.; Boggs, J. E. Cubic Force Constants and Equilibrium Geometry of Methane From Hartree–Fock and Correlated Wavefunctions. *J. Chem. Phys.* **1978**, *68*, 5077–5085.

(16) Demaison, J. Experimental, Semi-Experimental and Ab Initio Equilibrium Structures. *Mol. Phys.* **2007**, *105*, 3109–3138.

(17) Piccardo, M.; Penocchio, E.; Puzzarini, C.; Biczysko, M.; Barone, V. Semi-experimental equilibrium structure determinations by employing B3LYP/SNSD anharmonic force fields: Validation and application to semirigid organic molecules. *J. Phys. Chem. A* **2015**, *119*, 2058–2082.

(18) Demaison, J.; Boggs, J. E.; Császár, A. G. *Equilibrium Molecular Structures: from Spectroscopy to Quantum Chemistry*; CRC Press, 2016.

(19) Vogt, N.; Demaison, J. *Equilibrium Structure of Free Molecules*; Springer, 2023.

(20) Mendolicchio, M.; Penocchio, E.; Licari, D.; Tasinato, N.; Barone, V. Development and Implementation of Advanced Fitting Methods for the Calculation of Accurate Molecular Structures. *J. Chem. Theory Comput.* **2017**, *13*, 3060–3075.

(21) Mendolicchio, M.; Barone, V. Unbiased Comparison Between Theoretical and Experimental Molecular Structures and Properties: Toward an Accurate Reduced-Cost Evaluation of Vibrational Contributions. *J. Chem. Theory Comput.* **2024**, *20*, 2842–2857.

(22) Knizia, G.; Adler, T. B.; Werner, H.-J. Simplified CCSD(T)-F12 methods: Theory and benchmarks. *J. Chem. Phys.* **2009**, *130*, 054104.

(23) Spackman, P. R.; Jayatilaka, D.; Karton, A. Basis Set Convergence of CCSD(T) Equilibrium Geometries Using a Large and Diverse Set of Molecular Structures . *J. Chem. Phys.* **2016**, *145*, 104101.

(24) Barone, V.; Crisci, L.; Di Grande, S. Accurate Thermochemical and Kinetic Parameters at Affordable Cost by Means of the Pisa Composite Scheme (PCS). *J. Chem. Theory Comput.* **2023**, *19*, 7273–7286.

(25) Di Grande, S.; Kàllay, M.; Barone, V. Accurate Thermochemistry at Affordable Cost by Means of an Improved Version of the JunChS-F12 Model Chemistry. *J. Comput. Chem.* **2023**, *44*, 2149–2157.

(26) Peterson, K. A.; Dunning Jr, T. H. Accurate Correlation Consistent Basis Sets for Molecular Core–Valence Correlation Effects: The Second Row Atoms Al–Ar, and the First Row Atoms B–Ne Revisited. *J. Chem. Phys.* **2002**, *117*, 10548–10560.

(27) Di Grande, S.; Barone, V. Toward Accurate Quantum Chemical Methods for Molecules of Increasing Dimension: the New Family of Pisa Composite Schemes. *J. Phys. Chem. A* **2024**, *128*, 4886–4900.

(28) Lazzari, F.; Di Grande, S.; Crisci, L.; Mendolicchio, M.; Barone, V. Molecular Structures With Spectroscopic Accuracy at DFT Cost by the Templating Synthon Approach and the PCS141 database. *J. Chem. Phys.* **2025**, *162*, 114310.

(29) Cordero, B.; Gomez, V.; Platero-Prats, A. E.; Revés, M.; Echevarria, J.; Cremades, E.; Barragan, F.; Alvarez, S. Covalent Radii Revisited. *Dalton Trans.* **2008**, 2832–2838.

(30) Barone, V. PCS/Bonds and PCS0: Pick Your Molecule and Get Its Accurate Structure and Ground State Rotational Constants at DFT Cost. *J. Chem. Phys.* **2023**, *159*, 081102.

(31) Santra, G.; Sylvetsky, N.; Martin, J. M. Minimally Empirical Double-Hybrid Functionals Trained Against the GMTKN55 Database: revDSD-PBEP86-D4, revDOD-PBE-D4, and DOD-SCAN-D4. *J. Phys. Chem. A* **2019**, *123*, 5129–5143.

(32) Grimme, S.; Ehrlich, S.; Goerigk, L. Effect of the Damping Function in Dispersion Corrected Density Functional Theory. *J. Comp. Chem.* **2011**, *32*, 1456–1465.

(33) Barone, V. From Perception to Prediction and Interpretation: Enlightening the Gray Zone of Molecular Bricks of Life With the Help of Machine Learning and Quantum Chemistry. *WIREs Comput. Mol. Sci.* **2025**, *15*, e:70000.

(34) Clark, T.; Chandrasekhar, J.; Spitznagel, G. W.; Schleyer, P. V. R. Efficient Diffuse Function-Augmented Basis Sets for Anion Calculations. III. The 3-21+G Basis Set for First-Row Elements, Li-F. *J. Comput. Chem.* **1983**, *4*, 294–301.

(35) Mendolicchio, M.; Barone, V. Accurate Vibrational and Ro-vibrational Contributions to the Properties of Large Molecules by a New Engine Employing Curvilinear Internal Coordinates and Vibrational Perturbation Theory to Second Order. *J. Chem. Theory Comput.* **2024**, *20*, 8378–8395.

(36) Uribe, L.; Lazzari, F.; Di Grande, S.; Crisci, L.; Mendolicchio, M.; Barone, V. Accurate Structures and Rotational Constants of Bicyclic Monoterpenes at DFT Cost by Means of the Bond-Corrected Pisa Composite Scheme (BPCS). *J. Chem. Phys.* **2024**, *161*, 014307.

(37) Lazzari, F.; Uribe, L.; Di Grande, S.; Crisci, L.; Mendolicchio, M.; Barone, V. Structures and Rotational Constants of Monocyclic Monoterpenes at DFT Cost by Pisa Composite Schemes and Vibrational Perturbation Theory. *J. Phys. Chem. A* **2025**, *129*, 503–517.

(38) Ray, B. S. Über die Eigenwerte des asymmetrischen Kreisels. *Zeitschr. Phys.* **1932**, *78*, 74–91.

(39) Plusquellic, D. F. JB95 Spectral fitting program. (accessed: 26.04.2025); `NISThttps://www.nist.gov/services-resources/software/jb95-spectral-fitting-program`.

(40) Cooke, S.; Ohring, P. Decoding Pure Rotational Molecular Spectra for Asymmetric Molecules. *J. Mol. Spectrosc.* **2013**, *2013*, 698392.

(41) Pickett, H. M. The Fitting and Prediction of Vibration-Rotation Spectra with Spin Interactions. *J. Mol. Spectrosc.* **1991**, *148*, 371–377.

(42) Kisiel, Z.; Pszczółkowski, L.; Medvedev, I. R.; Winnewisser, M.; De Lucia, F. C.; Herbst, E. Rotational Spectrum of Trans-Trans Diethyl Ether in the Ground and Three Excited Vibrational States. *J. Mol. Spectrosc.* **2005**, *233*, 231–243.

(43) Kisiel, Z. Software Packages for Broadband High-Resolution Spectroscopy. (accessed: 26.04.2025); `http://info.ifpan.edu.pl/~kisiel/prospe.htm#use`.

(44) Kisiel, Z. PROSPE - Programs for ROtational SPEctroscopy. (accessed: 26.04.2025); `https://www.ifpan.edu.pl/~kisiel/prospe.htm`.

(45) Watson, J. K. G. *Vibrational Spectra and Structure* **1977**, *6*, 1–87.

(46) Uribe, L.; Di Grande, S.; Crisci, L.; Lazzari, F.; Mendolicchio, M.; Barone, V. Accurate Structures and Rotational Constants of Steroid Hormones at DFT Cost: Androsterone, Testosterone, Estrone, β-Estradiol, and Estriol. *J. Phys. Chem. A* **2024**, *128*, 2629–2642.

(47) Sedo, G.; Marshall, F. E.; Grubbs II, G. S. Rotational Spectra of the Low Energy Conformers Observed in the (1R)-(-)-Myrtenol Monomer. *J. Mol. Spectrosc.* **2019**, *356*, 32–36.

(48) Neeman, E. M.; Osseiran, N.; Huet, T. The Conformational Landscape of Myrtenol: The Structure of the Hydroxymethyl Group and its Robustness Upon Hydration. *J. Chem. Phys.* **2022**, *156*, 124301.

(49) Di Grande, S.; Lazzari, F.; Barone, V. Accurate Geometries of Large Molecules at DFT Cost by Semiexperimental and Coupled Cluster Templating Fragments. *J. Chem. Theory Comput.* **2024**, *20*, 9243–9258.

TOC Graphic

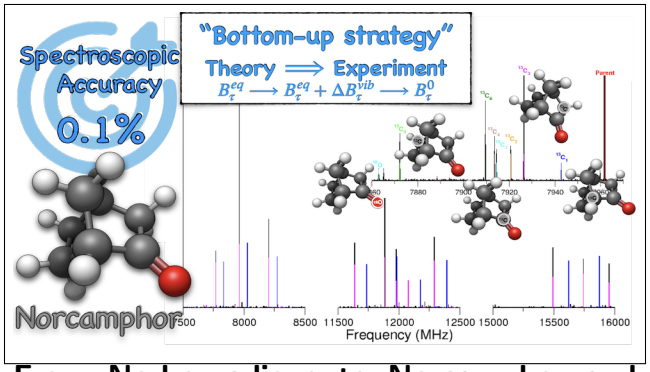

From Norbornadiene to Norcamphor and Camphor: Reduced-Cost Semiexperimental Structural Refinement from Limited Isotopologue Data